

ORIGINAL RESEARCH



Immune suppressive microenvironment in brain metastatic non-small cell lung cancer: comprehensive immune microenvironment profiling of brain metastases versus paired primary lung tumors (GASTO 1060)

Meichen Li^{a*}, Xue Hou^{a*}, Ke Sai^{b*}, Lihong Wu^{c*}, Jing Chen^a, Baishen Zhang^a, Na Wang^a, Lijia Wu^c, Hongbo Zheng^c, Jiao Zhang^c, Yonggao Mou^b, and Likun Chen^a

^aDepartment of Medical Oncology, Sun Yat-Sen University Cancer Center; State Key Laboratory of Oncology in South China; Collaborative Innovation Center for Cancer Medicine, Guangzhou, P. R. China; ^bDepartment of Neurosurgery, Sun Yat-Sen University Cancer Center; State Key Laboratory of Oncology in South China; Collaborative Innovation Center for Cancer Medicine, Guangzhou, P. R. China; ^cGenecast Biotechnology Co., Ltd, Wuxi, P.R. China

ABSTRACT

Lung cancer is one of the most common causes of brain metastases and is always associated with poor prognosis. We investigated the immunophenotypes of primary lung tumors and paired brain metastases, as well as immunophenotypes in the synchronous group (patients with brain metastases upon initial diagnosis) and metachronous group (patients developed brain metastases during the course of their disease). RNA sequencing of eighty-six samples from primary lung tumors and paired brain metastases of 43 patients was conducted to analyze the tumor immune microenvironment. Our data revealed that matched brain metastases compared with primary lung tumors exhibited reduced tumor infiltrating lymphocytes (TILs), a higher fraction of neutrophils infiltration, decreased scores of immune-related signatures, and a lower proportion of tumor microenvironment immune type I (high PD-L1/high CD8A) tumors. Additionally, we found a poor correlation of PD-L1 expression between paired brain metastases and primary lung tumors. In addition, gene set enrichment analysis (GSEA) showed that some gene sets associated with the immune response were enriched in the metachronous group, while other gene sets associated with differentiation and metastasis were enriched in the synchronous group in the primary lung tumors. Moreover, the tumor immune microenvironment between paired brain metastases and primary lung tumors displayed more differences in the metachronous group than in the synchronous group. Our work illustrates that brain metastatic tumors are more immunosuppressed than primary lung tumors, which may help guide immunotherapeutic strategies for NSCLC brain metastases.

ARTICLE HISTORY

Received 5 July 2021
Revised 24 March 2022
Accepted 25 March 2022

KEYWORDS

Brain metastases; non-small cell lung cancer; immune microenvironment; immunotherapy





Introduction

Lung cancer is one of the most common causes of brain metastases (BMs) and is always associated with poor prognosis.¹ In the last decades, the patients with brain metastases have been increasing due to the advancements in neuroimaging and systemic treatment.^{2,3} Patients with identified of brain metastases at their initial diagnosis were classified as synchronous brain metastases. The other part of patients who developed brain metastases during or after treatment for primary cancers were classified as metachronous brain metastases.^{2,4} In previous studies, patients with metachronous brain metastases manifested different clinicopathologic characteristics and have more favorable prognosis compared to synchronous brain metastases.⁵⁻⁷ Besides, the study for brain metastases of clear-cell renal-cell carcinoma showed that metachronous and synchronous groups harbor different chromosomal aberrations and mutational patterns, with significant inferior outcomes in the synchronous brain metastases.⁸ Thus, whether synchronous and


metachronous brain metastases represent different subtypes with respect to their biological behavior is imperative as it might have significance in clinical practice.

Recent studies have revealed that immune checkpoint inhibitors (ICIs) are promising effective treatments for various advanced cancer types, and ICI combination strategies have become the standard first-line treatment for advanced non-small cell lung cancer (NSCLC) without driver mutations.⁹⁻¹¹ However, for patients with brain metastases, the evidence for immune checkpoint inhibitor efficacy has been limited to subgroup or retrospective analyses, and their intracranial efficacy has not yet been fully validated.^{12,13}

Various biomarkers have been reported to be associated with the efficacy of immune checkpoint inhibitors, including tumor-infiltrating lymphocytes (TILs), tumor mutation burdens, PD-L1 expression, and other immune-related gene expression.¹⁴ Compared to extracranial tissues, there are distinctive tissue-resident cell types, such as microglia, astrocytes,

CONTACT Likun Chen  chenlk@sysucc.org.cn  Department of Medical Oncology, Sun Yat-Sen University Cancer Center; State Key Laboratory of Oncology in South China; Collaborative Innovation Center for Cancer Medicine, Guangzhou, P. R. China; Yonggao Mou  mouyg@sysucc.org.cn  Department of Neurosurgery, Sun Yat-Sen University Cancer Center; State Key Laboratory of Oncology in South China; Collaborative Innovation Center for Cancer Medicine, Guangzhou, P. R. China

*These authors contributed equally to this work

 Supplemental data for this article can be accessed on the [publisher's website](#)

© 2022 The Author(s). Published with license by Taylor & Francis Group, LLC.

This is an Open Access article distributed under the terms of the Creative Commons Attribution-NonCommercial License (<http://creativecommons.org/licenses/by-nc/4.0/>), which permits unrestricted non-commercial use, distribution, and reproduction in any medium, provided the original work is properly cited.

and neurons, in the brain microenvironment. The brain is considered a specific immune-privileged organ and can be sheltered from immune surveillance and attack by the blood-brain barrier (BBB).¹⁵ However, Antoine et al. recently reported functional lymphatic vessels in the dural sinuses of mice.¹⁶ Furthermore, in brain tumors, the blood-brain barrier is often destroyed, and there can be an abundant infiltration of immune cells from the peripheral circulation.¹⁷ A better understanding of the intracranial immune microenvironment might contribute to the exploration of biomarkers for immunotherapy and novel therapeutic options for patients with brain metastases. Several studies have reported significant differences between primary tumors and brain metastases in the tumor microenvironment.^{18,19} However, previous studies had limited sample sizes, and the results were controversial. The tumor immune microenvironment between the metachronous and synchronous groups has not been investigated as well. Additional studies including larger patient cohorts need to be performed. In this study, we enrolled a cohort of 43 patients with NSCLC brain metastases to perform a comprehensive tumor microenvironment analysis between primary lung tumors and paired brain metastasis tumors.

Materials and methods

Patients

Forty-three Chinese patients with NSCLC who had brain metastasis at presentation or during the course of their disease were admitted to the Sun Yat-Sen University Cancer Center (Guangzhou, China) from 2000 to 2019, and they were retrospectively studied in this report. Archived, formalin-fixed, paraffin embedded (FFPE), surgically resected primary lung tumors and paired BM samples were available for all patients. Brain metastasis was identified by a pathologist and confirmed by magnetic resonance imaging. The clinical characteristics of the 43 patients are summarized in Table 1. This study was approved by the Guangdong Association Study of Thoracic Oncology (identifier GASTO 1060) and were performed in accordance with the Declaration of Helsinki. At the time of sample collection, all patients provided informed written consent to participate in the study.

RNA sequencing and sequencing data processing

Total RNA was extracted from FFPE samples using a RNeasy FFPE Kit (Qiagen) according to the manufacturer's instructions. The RNA was quantified on a Qubit 3.0/4.0 (Life Invitrogen) and assessed on a 2100 Bioanalyzer (Agilent). Then, 50 ng of total RNA was used with the SMARTer Stranded Total RNA-Seq Kit v2 (Takara) in accordance with the low-throughput protocol. After PCR enrichment and purification of adapter-ligated fragments, RNA-seq libraries were paired-end sequenced using the Illumina NovaSeq 6000 Sequencing System.

To ensure data quality, raw reads were preprocessed by removing adaptor sequences and low-quality reads using Trimmomatic (version 0.36),²⁰ RSeQC (version 2.6.4)²¹ and bowtie2 (version 2.3.4.1)²² by using default parameters

to obtain high-quality sequences (clean reads), and all subsequent analyses were based on clean reads. Reference gene and genome annotation files were downloaded from the GENCODE website (<https://www.genecodegenes.org/human/>). Clean data were aligned to the reference genome (GRCh37.p13.genome) by HISAT (version 2.1.0).²³ FeatureCounts²⁴ was used to estimate the expression level of each gene by using default parameters. The quantification of gene expression was performed using the TPM (transcripts per million) method. All the sequencing data used in this study passed the quality control, with clean data > 3 G, and uniquely mapping rate > 60%.

Differential Gene Expression Analysis

The input data for differential gene expression analysis were read counts from gene expression level analysis. The DESeq2 (version 1.20.0)²⁵ package in R software (version 3.6.3) was used to screen differentially expressed genes between comparisons. Data were normalized by a negative binomial distribution statistical method. The resulting P values were subjected to multiple test corrections according to the Benjamini and Hochberg methods to exclude false positives. The differentially expressed genes were identified when adjusted P value < 0.05 and $|\log_2(\text{Fold Change})| > 1$

Gene Set Enrichment Analysis

Gene Set Enrichment Analysis (GSEA) (<http://software.broadinstitute.org/gsea/index.jsp>)²⁶ (version gsea-3.0.jar) was conducted based on the expression results by using default parameters on C5 gene sets in the Molecular Signatures Database (MSigDB) (<http://software.broadinstitute.org/gsea/msigdb>) (version v6.2). GSEA analyzed ranked gene lists using a permutation-based test. GSEA plots, ES (enrichment score), NES (normalized enrichment score), nominal p-value and FDR q-value are shown in the enrichment results.

Immune cell infiltration analysis

Single-sample gene set enrichment analysis (ssGSEA) (R library GSVA, method = "ssgsea")²⁷ was used to quantify the relative infiltration of 28 immune cell types in the tumor microenvironment. Feature gene panels for each immune cell type were obtained from a recent publication,²⁸ and were provided in Table S1. QuantIseq, (R library IOBR, method = "quantiseq")^{29,30} was used to estimate the absolute proportions of 10 immune cell types in samples based on the expression data.

Immune gene signatures calculation

The gene sets utilized for the immune signature score are presented in supplemental Table S2. These gene sets were defined as previously reported.^{28,31–33} For each patient, the signature score was calculated as the mean of the expression levels $[\log_2(\text{TPM}+1)]$ of the included genes.

Table 1. Clinical characteristics of patients used in this study.

Characteristic	Total	Synchronous (n = 15)	Metachronous (n = 28)	P value*
Gender, No. (%)				1
Male	29 (67.4)	10	19	
Female	14 (32.6)	5	9	
Age, No. (%)				0.835
≥60 y	21 (48.8)	7	14	
<60 y	22 (51.2)	8	14	
Age, median (range), y	58 (29–72)	52 (29–70)	59 (33–72)	
Smoking history, No. (%)				0.543
Smoker	26 (60.5)	10	16	
Never smoker	17 (39.5)	5	12	
KPS score, median (range)	90 (80–100)	90 (80–90)	90 (90–100)	
Histology, No. (%)				0.84
Adenocarcinoma	34 (79.1)	11	23	
Squamous cell carcinoma	4 (9.3)	2	2	
Adenosquamous carcinoma	2 (4.7)	1	1	
Others	3 (7.0)	1	2	
Stage at initial diagnosis, No. (%)				< 0.001
I–III	25 (58.2)	0	25	
IV	17 (39.5)	15	2	
NA	1 (2.3)	0	1	
Interval time between operation for lung cancer and diagnosis of brain metastases, median (range), day	380 (163–2888)	0	622 (163–2888)	
Treatment before brain surgery, No.				
Chemotherapy	19	0	19	
Targeted therapy	5	1	4	
Radiotherapy	1	0	1	
No systemic treatment	19	14	5	

* Chi-square test was used to calculate the p-values.

Normal lung and brain tissues expression data collection and processing

The gene expression data of normal lung and brain tissues were obtained from the Genotype-Tissue Expression (GTEx) portal (<https://gtexportal.org/>), including 288 normal lung tissues and 1141 normal brain tissues. Detailed sample information we used from GTEx is shown in Table S3. The immune cell infiltration analysis and immune gene signatures calculation of the normal lung and brain tissues were calculated as well as paired BM and primary lung tumors mentioned above.

Statistical analysis

All statistical analyses were performed using R software, version 3.6.3. The paired Wilcoxon signed-rank test or the Wilcoxon rank-sum test was carried out to compare values of immunological characteristics between paired comparisons or independent comparisons, and the resulting P values were adjusted with Benjamini and Hochberg (BH) method for multiple testing to minimize false positives. The chi-square test was used to test the association between two categorical variables. Pearson correlation was used to test the correlation of PD-L1 expression between paired brain metastases and primary lung tumors. All P-values were two-sided, and P-values of < 0.05 denoted statistical significance.

Results

Patients' characteristics

The clinicopathological characteristics of 43 Chinese patients with NSCLC are summarized in Table 1. This cohort included 29 male and 14 female patients, with a median age of 58 years.

In this cohort, 26 patients (60.5%) were smokers. Adenocarcinoma (n = 34 [79.1%]) was the most common histological subtype of primary NSCLC confirmed upon the initial diagnosis. Fifteen patients (35%) had synchronous metastatic brain tumors at the diagnosis of their primary NSCLC and were defined as the synchronous group. These patients underwent concurrent resection of the primary lung tumor and brain metastases at their initial diagnosis. Whereas the remaining twenty-eight patients (65%) developed brain metastasis during the course of their disease and were defined as the metachronous group. All patients in the synchronous group had stage IV disease, whereas patients in the metachronous group exhibited stage I to III disease ($P < .001$). The median interval time between surgery for lung cancer and the diagnosis of brain metastases in the metachronous group was 622 days (complete range 163–2888 days). In metachronous group, no patients received neoadjuvant therapy for primary tumors prior to surgical resection. Besides, there were nineteen patients received adjuvant chemotherapy, four patients received adjuvant targeted therapies with tyrosine kinase inhibitors (TKIs), and one patient received the intracranial radiotherapy before brain surgery in metachronous group.

Immune suppressive microenvironment in brain metastases

To comparatively characterize the immunological characteristics of the tumor microenvironment in brain metastases and primary lung tumors, we conducted RNA sequencing (RNA-seq) of 86 paired brain metastases and primary lung tumors from 43 patients. We first quantified the relative infiltration of 28 immune cell subtypes in the tumor microenvironment using single-sample gene set enrichment analysis (ssGSEA).²⁶

The relative abundance of each immune cell subtype was represented by an enrichment score in ssGSEA. We found that the enrichment score of each immune cell subtype was significantly lower in brain metastases than in paired primary lung tumors (Figure 1a). In order to check whether the observed differences were attributed to tissue type, we obtained the gene expression data of 1141 normal brain tissue samples and 288 normal lung tissue samples from Genotype-Tissue Expression (GTEx) data portal. The enrichment scores of 28 immune cell subtypes of normal brain and normal lung tissues were also calculated using ssGSEA. We found that there was no significant difference in the enrichment scores of immune cell subtypes between normal brain and normal lung tissues samples (Figure S1). So, the results we found in ssGSEA TIL infiltration were tumor-dependent. We then asked whether there were differences in the cell composition of the immune infiltrate between paired brain metastases and primary lung tumors. We used quanTIseq, a deconvolution-based method, to estimate cell fractions of 10 relevant infiltrating immune cells relative to the total amount of sequenced cells in samples. The differences of cell fraction of infiltrating immune cells between brain metastases and primary lung tumors were shown in Figure 1b. Higher fractions of neutrophils, CD4 T cells, and dendritic cells, and lower fractions of M1 macrophages and Tregs were observed in brain metastases. Similarly, we also analyzed the differences of cell fraction between normal brain and normal lung tissues, and found there were significant differences in cell fraction of 7 infiltrating immune cells between normal brain and normal lung tissues (Figure S2). It's worth noting that, comparing with normal lung tissues, the fraction of neutrophils was significantly lower in normal brain tissues, while the result of neutrophils in brain metastases was the opposite of those from normal brain tissues (Figure 1c), which revealed the findings of neutrophils infiltration in paired brain metastases and primary lung tumors were tumor-dependent, not tissue-dependent.

It has been reported that some predetermined sets of genes, including MHC molecules (class I, class II, and non-classical), immunoinhibitors signature, immunocostimulators signature, chemokines signature, adhesion molecules signature, cytolytic activity signature, IFN gamma signature and T cell-inflamed gene expression profiles (GEP) signature, are determinants of tumor immunogenicity and predictors of response to immune checkpoint blockade.^{28,31,33} Here, we used these ten immune-related gene signatures to evaluate the tumor immune environments (gene list of each signature see Table S2). Compared with the primary lung tumors, the expression scores of immune signatures, including the non-classical MHC signature, adhesion molecules signature, IFN gamma signature and T cell-inflamed GEP signature, were significantly lower in brain metastases ($P < .05$) (Figure 2a). We also examined the expression scores of immune signatures in normal brain and normal lung tissues, and found there were no significant differences in all ten immune signatures between normal brain and normal lung tissues (Figure S3).

In addition, we also analyzed the differential expression of immune inhibitory checkpoint molecules between paired brain metastases and primary lung tumors and found that the expression of C10orf54 (VISTA) and CTLA4 was

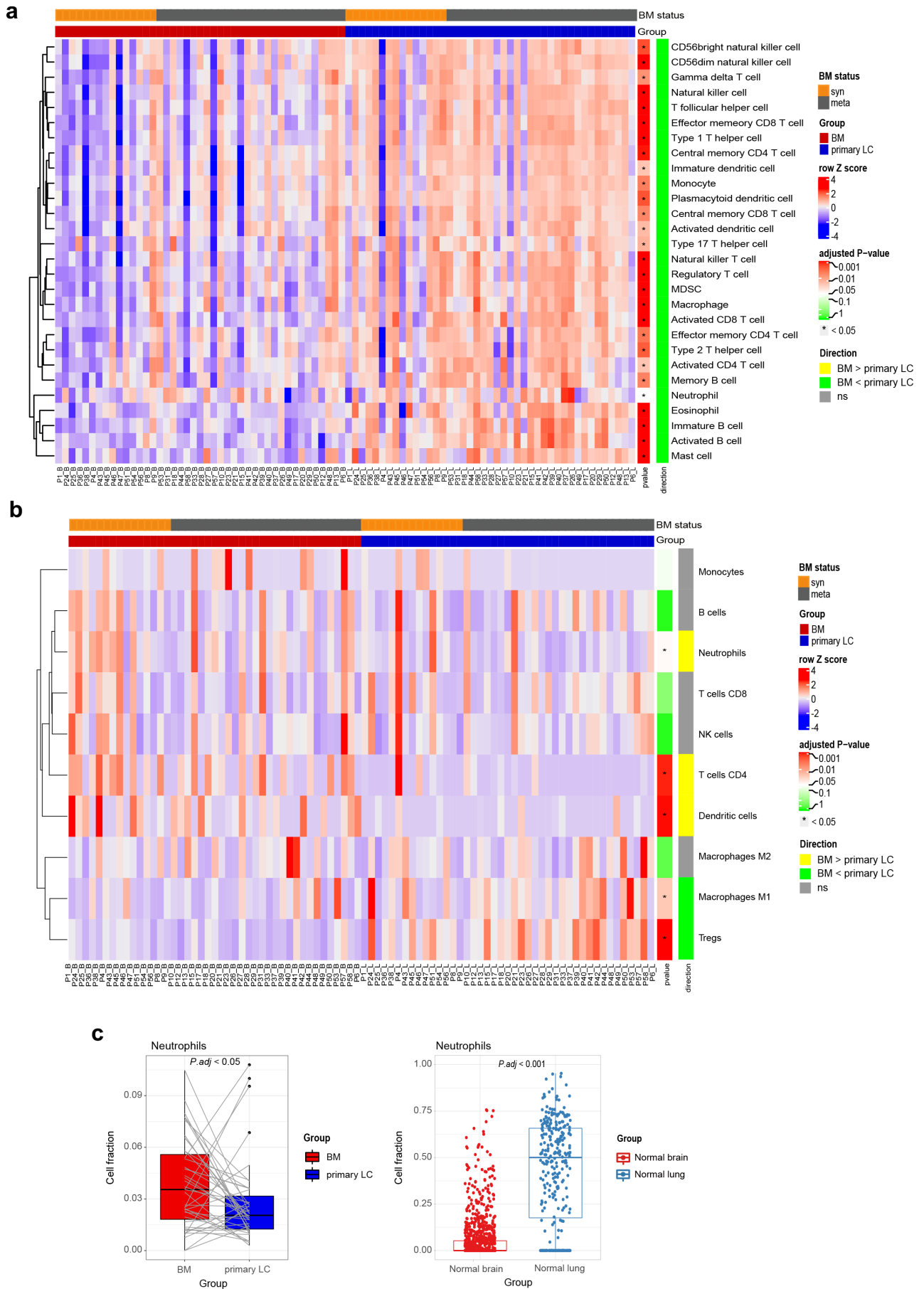
downregulated in brain metastases compared with primary lung tumors (Figure 2b). Furthermore, we checked the correlation of PD-L1 expression between brain metastases and primary lung tumors and found that there was a poor correlation of PD-L1 expression between paired brain metastases and primary lung tumors (Pearson $R = 0.25$, $P = .10$) (Figure 2c).

The classification of tumors into four different types based on the presence or absence of CD8+ CTLs and PD-L1 expression was recently suggested. Tumors with high PD-L1 expression and the presence of CD8+ CTLs in the microenvironment were classified as TME immune type I, and patients with this type would benefit from anti-PD-L1/PD-1 therapies.^{34,35} Here, we classified our cohort into four TME immune types (TMIT) according to the median values of PD-L1 and CD8A expression, as previously reported³⁴ (Figure S4, 2d). We found that the distributions of TMIT in brain metastases and primary lung tumors were different. The proportions of TMIT I (high PD-L1/high CD8A), TMIT II (low PD-L1/low CD8A), TMIT III (high PD-L1/low CD8A) and TMIT IV (low PD-L1/high CD8A) in brain metastases were 23%, 40%, 19%, and 19%, respectively, while those in primary lung tumors were 47%, 30%, 12%, and 12%, respectively. Brain metastases contained a significantly lower proportion of TMIT I than primary lung tumors (Figure 2d). Overall, these data indicated that brain metastases display a suppressed immune microenvironment compared with primary lung tumors.

Immunological characteristics in the synchronous group and metachronous group of primary lung tumors

The patients with brain metastases could be divided into a synchronous metastatic group and a metachronous metastatic group according to the pattern of brain metastases. However, little is known about the differences in the immune microenvironment between synchronous and metachronous primary lung tumors. Here, we compared the gene expression profiles of primary lung tumors between the synchronous group ($n = 15$) and metachronous group ($n = 28$). The differentially expressed genes were identified when adjusted P value $< .05$ and $|\log_2(\text{Fold Change})| > 1$. We found that only one gene, ALB (albumin), was significantly overexpressed in the synchronous group, and none of the immune-related genes were differentially expressed in primary lung tumors between the synchronous group and metachronous group (data not shown). We then used gene set enrichment analysis (GSEA) to identify gene sets whose expression were enriched or depleted in the metachronous group versus the synchronous group. Some gene sets showing upregulation in the metachronous group versus the synchronous group were implicated in the immune response, such as regulation of type I interferon production, regulation of interferon alpha production and T cell homeostasis, while the gene sets associated with differentiation and metastasis were downregulated in the metachronous group versus the synchronous group (Figure 3a).

TIL infiltration analysis using ssGSEA approach and quanTIseq approach all showed that there was no significant difference in the infiltrating immune cell subtypes between metachronous group and synchronous group (Figure S5, Figure 3b). Additionally, immune gene signature analysis



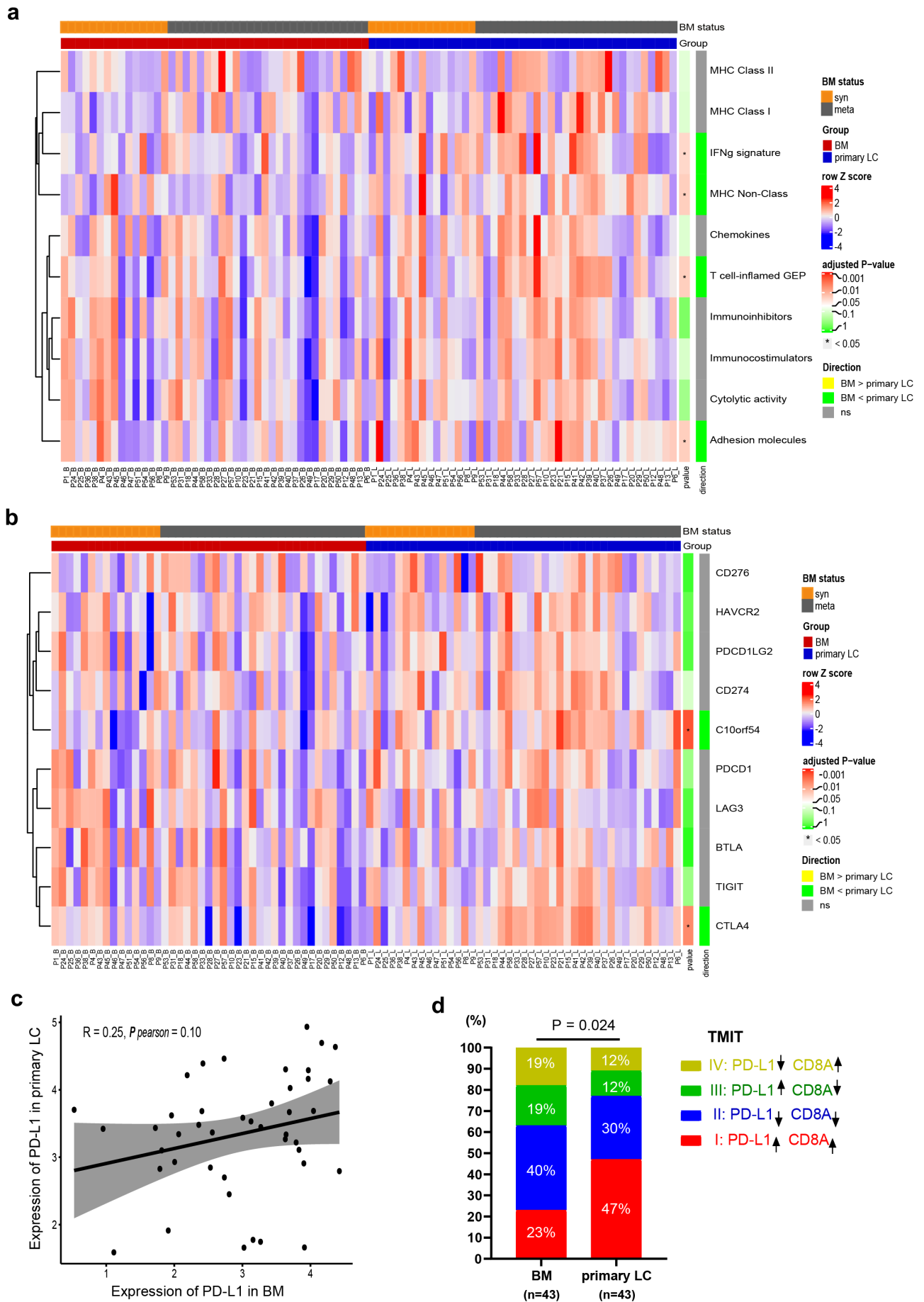
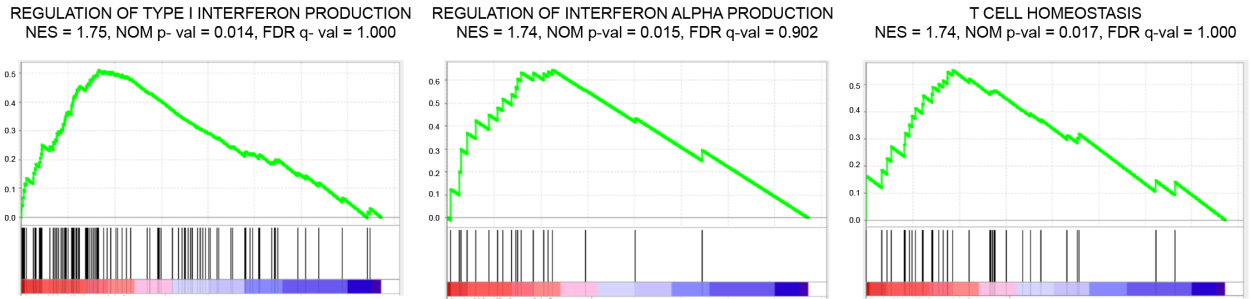


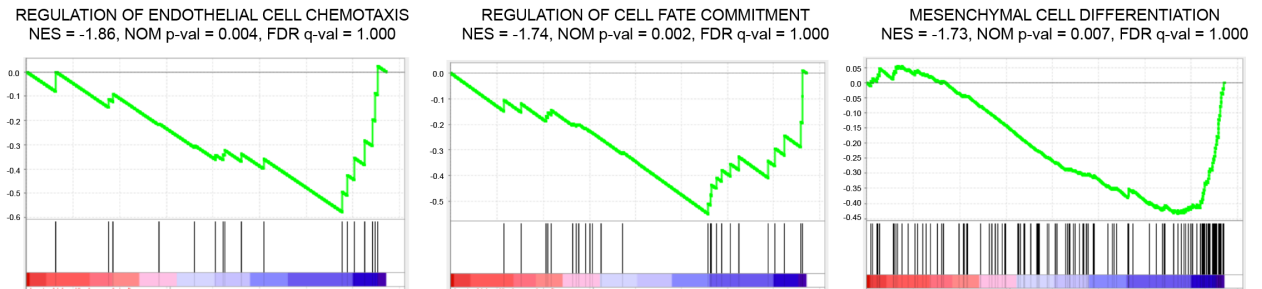
Figure 2. Comparison of immune characteristics between paired brain metastases and primary lung tumors.

a

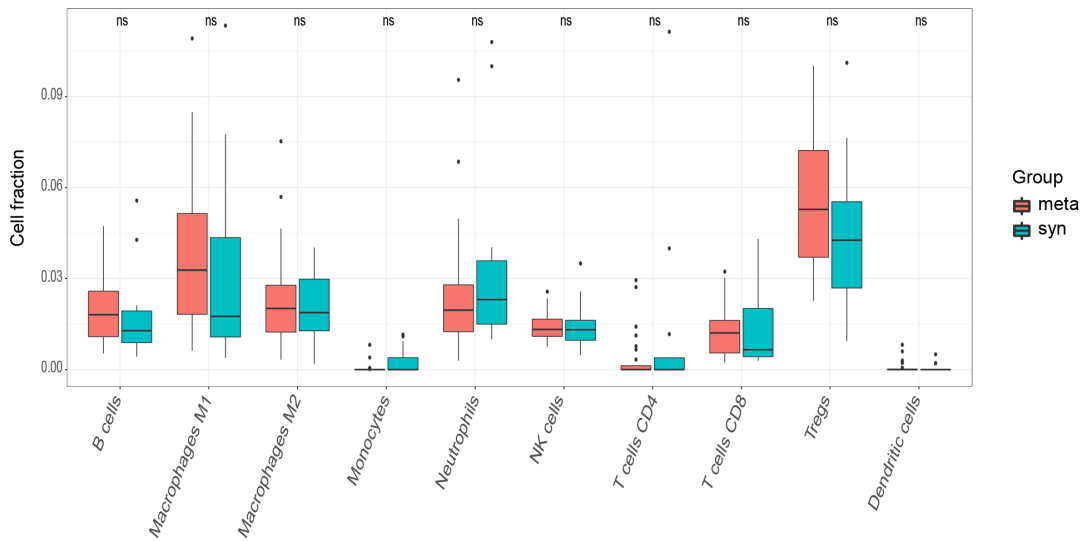
Pathways enriched in tumors with metachronous group



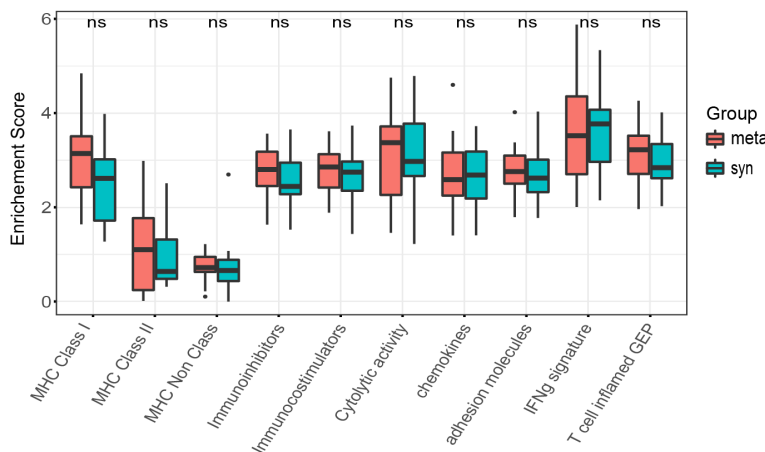
Pathways depleted in tumors with metachronous group



b



c



d

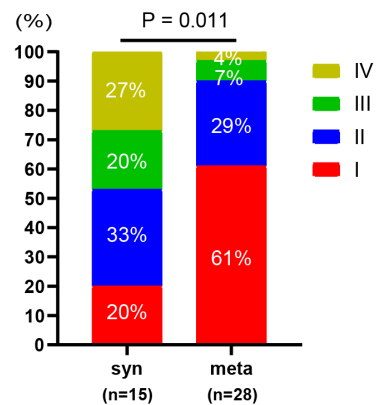


Figure 3. Comparison of immunological characteristics between synchronous group and metachronous group in primary lung tumors.

showed that none of immune signature scores were significantly changed in the metachronous group versus the synchronous group (Figure 3c). TMIT analysis suggested that the proportion of TMIT I (CD8A high, PD-L1 high) was elevated in the metachronous group compared to the synchronous group ($P = .011$) (Figure 3d). These results implied that the tumor immune microenvironment in the synchronous group might be statistically comparable to those in the metachronous group in primary lung tumors.

Immunological characteristics between paired brain metastases and primary lung tumors in the synchronous group and metachronous group

According to the pattern of brain metastases, all the patients in this cohort could be divided into a synchronous group and a metachronous group. We next checked whether there were differences in the immunological characteristics described above between the paired brain metastases and primary lung tumors in these two groups. We found there were differences in the TILs infiltration in these two groups. The ssGSEA results showed that only activated B cell and mast cell were significantly less abundant in brain metastases in the synchronous group, while the majority of the 28 immune cell subtypes were significantly less abundant in brain metastases in the metachronous group (Figure S6). The quanTIseq results revealed that there was no significant difference in the cell fraction between the paired brain metastases and primary lung tumors in the synchronous group after multiple tests, while there were several differences in the cell fraction between the paired brain metastases and primary lung tumors in the metachronous group (Figure 4a), including higher fractions of monocytes, CD4 T cells, and dendritic cells, and lower fractions of M1 macrophages and Tregs in brain metastases. Interestingly, the expression scores of the immune signatures described above also exhibited differences between the paired brain metastases and primary lung tumors in these two groups. In the synchronous group, there was no significant difference in the scores of all ten immune signatures between paired brain metastases and the primary lung tumors (Figure 4b). In contrast, the scores of some immune signatures, including non-classical MHC signature, adhesion molecules signature, IFN-gamma signature and T cell-inflamed GEP signature, were significantly reduced in the brain metastases in the metachronous group (Figure 4b). Similarly, the expression of PD-L1 showed no correlation between paired brain metastases and primary lung tumors in the synchronous group ($R = 0.054$, $P = .85$) (Figure S7A), whereas there seemed to be a moderate correlation of PD-L1 expression between paired brain metastases and primary lung tumors in the metachronous group ($R = 0.38$, $P = .046$) (Figure S7B). The proportion of TMIT I (CD8A high, PD-L1 high) was not significantly different between the paired brain metastases and primary lung tumors in the synchronous group ($P = .213$) (Figure S8A), while it was significantly lower in brain metastases than in primary lung tumors in the metachronous group ($P < .001$) (Figure S8B). Overall, these

results suggested that the tumor immune microenvironment between paired brain metastases and primary lung tumors displayed more differences in the metachronous group than in the synchronous group.

Considering the adjuvant treatments following surgery may influence the immune microenvironment of metastases, we checked the effect of therapies on the immune profiles of brain metastases in the metachronous group. As we summarized in Table 1, there were nineteen patients received adjuvant chemotherapy, four patients received adjuvant targeted therapy, only one patient received radiotherapy before brain surgery, and five patients receive no systemic treatment in metachronous group. We compared the TILs infiltration and immune signatures expression in metachronous metastatic patients who received adjuvant chemotherapy and those who did not, and found that except the cell fraction of NK cells, no significant difference was found in the enrichment scores of immune cell subtypes, cell fractions of immune cell subtypes, and the expression scores of immune related signatures in brain metastases of metachronous group (Figure S9 A-C). Similarly, we did not find significant differences in the TIL infiltration and immune signatures expression in brain metastases of metachronous group between patients who received targeted therapy and those who did not, as well as patients who received the systemic therapy and those who did not (Figure S10, S11). There was a trend toward lower expression of cytolytic activity signature, chemokines signature, adhesion molecules signature and T cell-inflamed GEP signature in brain metastases of the patients who received targeted therapy. However, these significances disappeared after multiple tests (Figure S10C). Thus, our data showed that the impact of adjuvant therapy about metachronous group is relatively low.

Discussion

In this study, we comprehensively analyzed the tumor immune microenvironment of paired brain metastases and primary lesions from 43 NSCLC patients using an RNA sequencing platform. Our data showed that brain metastases compared with primary lung tumors had i) reduced TILs infiltration; ii) a higher fraction of neutrophils; iii) reduced expression scores of immune-related gene signatures (non-classical MHC signature, adhesion molecules signature, IFN gamma signature and T cell-inflamed GEP signature); iv) suppressed expression of immune checkpoint molecules (VISTA and CTLA4); and v) a lower proportion of TMIT I (high PD-L1 and high CD8A expression). Our work revealed that the brain tumors are further immunosuppressed compared with primary lung tumors, which indicates poor anti-tumor immune response and are related to tumor growth and metastases in previous study.³⁶

We used two methods to evaluate the immune cell infiltration in paired brain metastases and primary lung tumors. The ssGSEA estimated the relative enrichment of each cell type in samples from their gene expression profiles, but might fail to estimate the cell fractions of cell types in samples. We found that brain metastases exhibited a lower enrichment of total immune cells compared to primary lung tumors, which was in line with results presented in previous reports.^{37,38} In addition, we further used quanTIseq methods to compare the cell

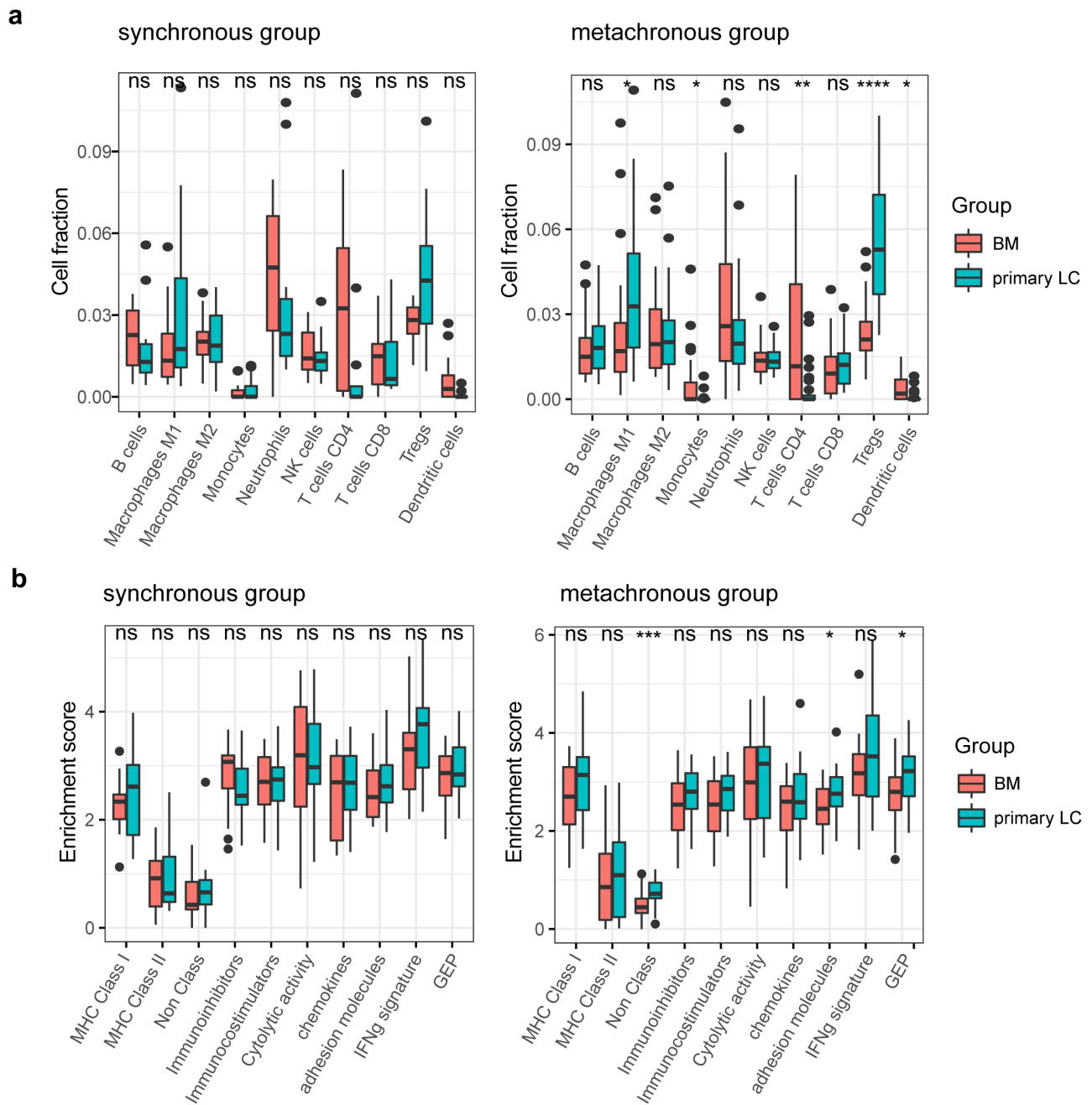


Figure 4. Comparison of immunological characteristics between paired brain metastases and primary lung tumors in synchronous group and metachronous group, respectively.

composition of immune infiltrations between the brain metastatic tumors and primary lung tumors, which was a deconvolution-based algorithm, to generate the absolute scores that can be interpreted as cell fractions and compared both inter- and intra-samples. An elevated fraction of neutrophils infiltration in brain tumors was observed in our study, which may exert main immunosuppressive roles in brain microenvironment and be correlated to brain metastasis. Neutrophils are most abundant innate immune cells in both bone marrow and peripheral blood,³⁹ several studies showed that tumor microenvironment may reprogram neutrophils and shift them to immunosuppressive phenotype.⁴⁰ Tumor-

associated neutrophils (TANs) promote cancer growth and metastasis by recruiting macrophages and Tregs, inhibiting cytotoxic T cells and natural killer cells, and promoting angiogenesis.^{41–43} And several studies have demonstrated that high neutrophil-to-lymphocyte ratio (NLR) is associated with poor outcomes in patients with brain metastases.^{44,45} Recently, various therapeutic approaches have been developed to inhibit or modulate the phenotype of neutrophils,⁴⁶ our findings of increased fraction of neutrophils infiltration in brain metastases suggest that targeting immunosuppressive TANs may be a feasible immunotherapeutic approach for the clinical management of brain metastases in NSCLC.

In this study, the expression scores of many immune-related signatures, including non-classical MHC signature and adhesion molecules signature, were decreased in brain metastases. These findings indicated that metastatic lung cancer cells might evade immune surveillance through multiple mechanisms, including reduced antigen presentation and downregulation of the expression of adhesion molecules, leading to an immune-cell-depleted microenvironment. The IFN-gamma signature and T cell-inflamed GEP signature are predictors of the clinical response to ICIs.³¹ Our results showed that the scores of the IFN-gamma signature and T cell-inflamed GEP signature were lower in brain metastases, indicating that the responsiveness to ICIs may differ between brain metastases and primary lung tumors, which was consistent with the results of the clinical trial of pembrolizumab for the management of patients with NSCLC and brain metastases.⁴⁷ The immunosuppressed tumor microenvironment of brain metastases highlights the need for new therapeutic strategies aimed at converting the immune-suppressive milieu into inflammatory environments. As the results of several studies have shown, radiotherapy may increase the release of damage-associated molecular patterns or stress molecules, the expression of MHC-I molecules for effective antigen presentation, the upregulation of PD-L1 expression on cancer cells, and blood-brain barrier permeability, allowing for better penetration of immune checkpoint inhibitors into the brain.^{48–52} Chemotherapy may indeed enhance the effect of ICIs by increasing T-cell responses and disrupting the activity of TAMs.⁵³ Combining immunotherapy with other forms of chemotherapy, radiotherapy may potentiate their effect in the setting of brain metastases. To date, a number of clinical trials have attempted to combine immunotherapeutic agents with other forms of therapy to achieve a breakthrough.⁵⁴

It has been proposed that four different types of tumor microenvironments exist based on the presence or absence of TILs and PD-L1 expression, which sheds light on new approaches for rationally designing ideal combination cancer therapies based on tumor immunology.³⁵ Ock et al. classified a large set of TCGA pan-cancer samples into four TME immune types (TMIT) by measuring the mRNA expression levels of PD-L1 and CD8A and found that TMIT I (PD-L1+/CD8A+) was associated with a high mutational burden, PD-L1 amplification, and oncogenic viral infection.³⁴ Our TMIT analysis showed that the proportion of TMIT I (high PD-L1/high CD8A expression) in brain metastases was significantly lower than that in primary lung tumors, indicating that the tumor microenvironment in brain metastases was immunosuppressed. Patients with TMIT I might be responders to immune checkpoint blockade therapy.

PD-L1 expression is commonly used to predict the response to immune checkpoint inhibitor therapy. However, the dynamics of PD-L1 expression may limit its use as a tissue-based predictive biomarker. We found that the expression of PD-L1 in brain metastases was poorly correlated with paired primary lung tumors. Our results were consistent with those of previous reports in which it was shown that there was temporal and spatial discordance of PD-L1 expression between paired primary lesions and brain metastases in lung cancer.¹⁹ Furthermore, our results

suggest that the responses to immunotherapy may be inconsistent between primary and metastatic lesions due to discrepancies in their tumor microenvironments. When physicians decide to treat patients with lung cancer with a PD-1 or PD-L1 inhibitor, they must consider the spatial and temporal heterogeneity of the tumor microenvironment.

Interestingly, we observed in this study that the tumor immune microenvironment between paired brain metastases and primary lung tumors displayed more differences in the metachronous group than in the synchronous group. And there was no significant difference in the expression scores of the immune signatures between brain metastases and primary lung tumors in synchronous group. Our results indicated that brain metastases in the synchronous group may produce an antitumor immune response similar to that of primary lung tumors. A similar phenomenon was also observed in other studies of metastatic cancers. Jiang et al. investigated the heterogeneity of the neoantigen landscape between primary lesions and their matched metastases in lung cancer and found that the counts, overall distribution pattern and predicted HLA binding affinity of neoantigens were similar between primary lesions and metastases.⁵⁵ All the samples they studied were collected before any systemic therapy, which was equivalent to the synchronous metastasis group. Shibutani et al. compared the local immune status between the primary and metastatic tumors in patients with stage IV colorectal cancer who underwent concurrent resection of the primary tumor and liver metastasis and found that the density of the TIL subsets, as well as the activation/suppression status of the lymphocytes of the primary tumor, were associated with that of the metastatic tumor.⁵⁶ Goto et al. found no significant difference in the number of FoxP3-positive tumor-infiltrating lymphocytes between right and left breast cancers in patients with synchronous bilateral breast cancer, where the tumors develop in the same host immune environment.⁵⁷ Chen et al. reported that patients with synchronous head and neck squamous cell carcinoma (HNSCC) and esophageal squamous cell carcinoma (ESCC) had significant higher CD8+ TILs in HNSCC and ESCC than metachronous patients. Furthermore, the immunologic expression was significantly correlated between the HNSCC and ESCC in synchronous patients.⁵⁸ There were differences in the immune microenvironment of synchronous and metachronous groups of brain metastases in NSCLC, suggesting that clinically different treatment decisions should be made for synchronous and metachronous brain metastases. However, more samples are needed to verify this result, and more corresponding mechanistic studies are necessary.

It has been reported that chemotherapy, radiotherapy, and chemoradiotherapy are able to alter the composition of the tumor immune microenvironment.⁵⁹ However, our data showed that the impact of adjuvant therapy about metachronous group is relatively low. In our cohort, for patients with metachronous brain metastases, the intracranial radiotherapy was mostly underwent followed by operation, except for one patient. So, the impact of radiotherapy on

the brain immune microenvironment may be relatively low. As for adjuvant therapy in metachronous group, there are nineteen patients received adjuvant chemotherapy and four patients received adjuvant targeted therapy. For patients received adjuvant chemotherapy, there are at least more than 6 months intervals between adjuvant chemotherapy and the occurrence of brain metastases. Recent studies have reported that the impact of chemotherapy and EGFR-TKI on the tumor immune microenvironment is temporary and disappeared as treatment continued in animal models.^{60–63} One study also reported that just one cycle of neoadjuvant chemotherapy induced an immune stimulatory microenvironment through serial tumor biopsies in breast cancer patients.⁶⁴ It would be better to evaluate the impact of treatment regimens on brain metastases in appropriate cohort in future.

There are several limitations that should be pointed out. First, the number of cases included in the current study is relatively small for reaching a solid conclusion. Second, it would be preferable to additionally analyze the tumor immune microenvironment of patients who received ICI treatment.

Conclusions

Our work illustrates the immune landscape of brain metastases from NSCLC and suggests that the tumor immune microenvironment in brain metastases compared with primary lung tumors is further immunosuppressed, which may help guide immunotherapeutic strategies for NSCLC brain metastases.

Acknowledgements

We would like to thank the patients and family members who gave their consent on presenting the data in this study, as well as the investigators and research staff involved in this study.

Authors' contributions

Meichen Li, Xue Hou, Yonggao Mou, and Likun Chen designed this study. Meichen Li, Xue Hou, Ke Sai, Jing Chen, Baishen Zhang and Na Wang collected the tissue samples and clinical data. Meichen Li, Lihong Wu, Lijia Wu, Hongbo Zheng, and Jiao Zhang performed the statistical analyses. Meichen Li, Lihong Wu, and Xue Hou drafted the manuscript. Yonggao Mou and Likun Chen provided critical comments and suggestions and revised the manuscript. All authors read and approved the final version of the manuscript.

Abbreviations

NSCLC:	non-small cell lung cancer;
FFPE:	formalin-fixed, paraffin embedded;
RNA-seq:	RNA sequencing;
TILs:	tumor infiltrating lymphocytes;
TMIT:	tumor microenvironment immune types;
BMs:	brain metastases;
ICI:	immune checkpoint inhibitor;
BBB:	blood-brain barrier;
TPM:	Transcripts Per Million;
GSEA:	Gene Set Enrichment Analysis;
ssGSEA:	single-sample gene set enrichment analysis;

GTEx:	Genotype-Tissue Expression;
GEP:	gene expression profile;
TME:	tumor microenvironment;
TAN:	tumor-associated neutrophil.

Ethics approval and consent to participate

The study was approved by the ethics committee of Guangdong Association Study of Thoracic Oncology (GASTO 1060) and were performed in accordance with the Declaration of Helsinki. All patients provided informed written consent to participate in the study.

Availability of data and material

Dr Chen had full access to all the data in the study and take responsibility for the integrity of the data and the accuracy of the data analysis. The RNA-seq data of paired brain metastases and primary lung tumors in this study have been uploaded to OMIX (<https://ngdc.cncb.ac.cn/omix/preview/Spec7IDiX>), with ID: OMIX575.

Disclosure statement

Lihong Wu, Lijia Wu, Hongbo Zheng, and Jiao Zhang are the employees of Genecast Biotechnology Co., Ltd, Wuxi. The other authors report no conflict of interest.

Funding

This work was supported by the National Natural Science Funds of China under Grant 82072559. The funding sources had no role in the design and conduct of the study; collection, management, analysis, and interpretation of the data; and decision to submit the manuscript for publication.

References

- Barnholtz-Sloan JS, et al. Incidence proportions of brain metastases in patients diagnosed (1973 to 2001) in the Metropolitan Detroit Cancer Surveillance System. *J Clin Oncol.* 2004;22(14):72–2865 doi:10.1200/JCO.2004.12.149.
- Jenkinson MD, Haylock B, Shenoy A, Husband D, Javadpour M. Management of cerebral metastasis: evidence-based approach for surgery, stereotactic radiosurgery and radiotherapy. *Eur J Cancer.* 2011;47(5):649–655. doi:10.1016/j.ejca.2010.11.033.
- Tabouret E, Chinot O, Metellus P, Tallet A, Viens P, Gonçalves A. Recent trends in epidemiology of brain metastases: an overview. *Anticancer Res.* 2012;32:4655–4662.
- Wronski M, Arbit E, Burt M, Galicich JH. Survival after surgical treatment of brain metastases from lung cancer: a follow-up study of 231 patients treated between 1976 and 1991. *J Neurosurg.* 1995;83(4):605–616. doi:10.3171/jns.1995.83.4.0605.
- Flannery TW, et al. Gamma knife stereotactic radiosurgery for synchronous versus metachronous solitary brain metastases from non-small cell lung cancer. *Lung Cancer.* 2003;42(3):327–333. doi:10.1016/S0169-5002(03)00357-X.
- Ashworth AB, Senan S, Palma DA, Riquet M, Ahn YC, Ricardi U, Congedo MT, Gomez DR, Wright GM, Melloni G, et al. An individual patient data metaanalysis of outcomes and prognostic factors after treatment of oligometastatic non-small-cell lung cancer. *Clin Lung Cancer.* 2014;15(5):346–355. doi:10.1016/j.clcc.2014.04.003.
- Chen K, et al. Lung-molGPA Index Predicts Survival Outcomes of Non-Small-Cell Lung Cancer Patients with Synchronous or Metachronous Brain Metastases. *Onco Targets Ther.* 2020;13:8837–8844. doi:10.2147/OTT.S255478.
- Gutenberg A, Nischwitz MD, Gunawan B, Enders C, Jung K, Bergmann M, Feiden W, Egensperger R, Keyvani K, Stolke D, et al. Predictive chromosomal clusters of synchronous and

- metachronous brain metastases in clear cell renal cell carcinoma. *Cancer Genet.* 2014;207(5):206–213. doi:10.1016/j.cancergen.2014.05.004.
9. Gandhi L, Rodriguez-Abreu D, Gadgeel S, Esteban E, Felip E, De Angelis F, Domine M, Clingan P, Hochmair MJ, Powell SF, et al. Pembrolizumab plus Chemotherapy in Metastatic Non-Small-Cell Lung Cancer. *N Engl J Med.* 2018;378(22):2078–2092. doi:10.1056/NEJMoa1801005.
 10. Paz-Ares L, et al. Pembrolizumab plus Chemotherapy for Squamous Non-Small-Cell Lung Cancer. *N Engl J Med.* 2018;379(21):2040–2051 doi:10.1056/NEJMoa1810865.
 11. West H, McCleod M, Hussein M, Morabito A, Rittmeyer A, Conter HJ, Kopp H-G, Daniel D, McCune S, Mekhail T, et al. Atezolizumab in combination with carboplatin plus nab-paclitaxel chemotherapy compared with chemotherapy alone as first-line treatment for metastatic non-squamous non-small-cell lung cancer (IMpower130): a multicentre, randomised, open-label, phase 3 trial. *Lancet Oncol.* 2019;20(7):924–937. doi:10.1016/S1470-2045(19)30167-6.
 12. Hendriks LEL, Henon C, Auclin E, Mezquita L, Ferrara R, Audigier-Valette C, Mazieres J, Lefebvre C, Rabeau A, Le Moulec S, et al. Outcome of Patients with Non-Small Cell Lung Cancer and Brain Metastases Treated with Checkpoint Inhibitors. *J Thorac Oncol.* 2019;14(7):1244–1254. doi:10.1016/j.jtho.2019.02.009.
 13. Schapira E, Hubbeling H, Yeap BY, Mehan WA, Shaw AT, Oh K, Gainor JF, Shih HA. Improved Overall Survival and Locoregional Disease Control With Concurrent PD-1 Pathway Inhibitors and Stereotactic Radiosurgery for Lung Cancer Patients With Brain Metastases. *Int J Radiat Oncol Biol Phys.* 2018;101(3):624–629. doi:10.1016/j.ijrobp.2018.02.175.
 14. Mazzaschi G, Madeddu D, Falco A, Bocchialini G, Goldoni M, Sogni F, Armani G, Lagrasta CA, Lorusso B, Mangiaracina C, et al. Low PD-1 Expression in Cytotoxic CD8+ Tumor-Infiltrating Lymphocytes Confers an Immune-Privileged Tissue Microenvironment in NSCLC with a Prognostic and Predictive Value. *Clin Cancer Res.* 2018;24(2):407–419. doi:10.1158/1078-0432.CCR-17-2156.
 15. Engelhardt B, Vajkoczy P, Weller RO. The movers and shapers in immune privilege of the CNS. *Nat Immunol.* 2017;18(2):123–131. doi:10.1038/ni.3666.
 16. Louveau A, Smirnov I, Keyes TJ, Eccles JD, Rouhani SJ, Peske JD, Derecki NC, Castle D, Mandell JW, Lee KS, et al. Structural and functional features of central nervous system lymphatic vessels. *Nature.* 2015;523(7560):337–341. doi:10.1038/nature14432.
 17. Weiss N, Miller F, Cazaubon S, Couraud P-O. The blood-brain barrier in brain homeostasis and neurological diseases. *Biochim Biophys Acta.* 2009;1788(4):842–857. doi:10.1016/j.bbamem.2008.10.022.
 18. Kim R, Keam B, Kim S, Kim M, Kim SH, Kim JW, Kim YJ, Kim TM, Jeon YK, Kim D-W, et al. Differences in tumor microenvironments between primary lung tumors and brain metastases in lung cancer patients: therapeutic implications for immune checkpoint inhibitors. *BMC Cancer.* 2019;19(1):19. doi:10.1186/s12885-018-5214-8.
 19. Mansfield AS, Aubry MC, Moser JC, Harrington SM, Dronca RS, Park SS, Dong H. Temporal and spatial discordance of programmed cell death-ligand 1 expression and lymphocyte tumor infiltration between paired primary lesions and brain metastases in lung cancer. *Ann Oncol.* 2016;27(10):1953–1958. doi:10.1093/annonc/mdw289.
 20. Bolger AM, Lohse M, Usadel B. Trimmomatic: a flexible trimmer for Illumina sequence data. *Bioinformatics.* 2014;30(15):2114–2120. doi:10.1093/bioinformatics/btu170.
 21. Wang L, Wang S, Li W. RSeQC: quality control of RNA-seq experiments. *Bioinformatics.* 2012;28(16):2184–2185. doi:10.1093/bioinformatics/bts356.
 22. Langmead B, Salzberg SL. Fast gapped-read alignment with Bowtie 2. *Nat Methods.* 2012;9(4):357–359. doi:10.1038/nmeth.1923.
 23. Kim D, Langmead B, Salzberg SL. HISAT: a fast spliced aligner with low memory requirements. *Nat Methods.* 2015;12(4):357–360. doi:10.1038/nmeth.3317.
 24. Liao Y, Smyth GK, Shi W. featureCounts: an efficient general purpose program for assigning sequence reads to genomic features. *Bioinformatics.* 2014;30(7):923–930. doi:10.1093/bioinformatics/btt656.
 25. Love MI, Huber W, Anders S. Moderated estimation of fold change and dispersion for RNA-seq data with DESeq2. *Genome Biol.* 2014;15(12):550. doi:10.1186/s13059-014-0550-8.
 26. Subramanian A, Tamayo P, Mootha VK, Mukherjee S, Ebert BL, Gillette MA, Paulovich A, Pomeroy SL, Golub TR, Lander ES, et al. Gene set enrichment analysis: a knowledge-based approach for interpreting genome-wide expression profiles. *Proc Natl Acad Sci U S A.* 2005;102(43):15545–15550. doi:10.1073/pnas.0506580102.
 27. Hanzelmann S, Castelo R, Guinney J. GSEA: gene set variation analysis for microarray and RNA-seq data. *BMC Bioinform.* 2013;14:7.
 28. Charoentong P, Finotello F, Angelova M, Mayer C, Efremova M, Rieder D, Hackl H, Trajanoski Z. Pan-cancer Immunogenomic Analyses Reveal Genotype-Immunophenotype Relationships and Predictors of Response to Checkpoint Blockade. *Cell Rep.* 2017;18(1):248–262. doi:10.1016/j.celrep.2016.12.019.
 29. Zeng D, et al. IOBR: multi-Omics Immuno-Oncology Biological Research to Decode Tumor Microenvironment and Signatures. *Front Immunol.* 2021;12:687975. doi:10.3389/fimmu.2021.687975.
 30. Finotello F, Mayer C, Plattner C, Laschober G, Rieder D, Hackl H, Krogsdam A, Loncova Z, Posch W, Wilflingseder D, et al. Molecular and pharmacological modulators of the tumor immune contexture revealed by deconvolution of RNA-seq data. *Genome Med.* 2019;11(1):34. doi:10.1186/s13073-019-0638-6.
 31. Ayers M, Lunceford J, Nebozhyn M, Murphy E, Loboda A, Kaufman DR, Albright A, Cheng JD, Kang SP, Shankaran V, et al. IFN-gamma-related mRNA profile predicts clinical response to PD-1 blockade. *J Clin Invest.* 2017;127(8):2930–2940. doi:10.1172/JCI91190.
 32. Davoli T, et al. Tumor aneuploidy correlates with markers of immune evasion and with reduced response to immunotherapy. *Science.* 2017;355:6322. doi:10.1126/science.aaf8399.
 33. Rooney MS, Shukla S, Wu C, Getz G, Hacohen N. Molecular and genetic properties of tumors associated with local immune cytolytic activity. *Cell.* 2015;160(1–2):48–61. doi:10.1016/j.cell.2014.12.033.
 34. Ock CY, Keam B, Kim S, Lee J-S, Kim M, Kim TM, Jeon YK, Kim D-W, Chung DH, Heo DS, et al. Pan-Cancer Immunogenomic Perspective on the Tumor Microenvironment Based on PD-L1 and CD8 T-Cell Infiltration. *Clin Cancer Res.* 2016;22(9):2261–2270. doi:10.1158/1078-0432.CCR-15-2834.
 35. Teng MW, Ngiow SF, Ribas A, Smyth MJ. Classifying Cancers Based on T-cell Infiltration and PD-L1. *Cancer Res.* 2015;75(11):2139–2145. doi:10.1158/0008-5472.CAN-15-0255.
 36. Hamada T, Soong TR, Masugi Y, Kosumi K, Nowak JA, da Silva A, Mu XJ, Twombly TS, Koh H, Yang J, et al. TIME (Tumor Immunity in the MicroEnvironment) classification based on tumor CD274 (PD-L1) expression status and tumor-infiltrating lymphocytes in colorectal carcinomas. *Oncoimmunology.* 2018;7(7):e1442999. doi:10.1080/2162402X.2018.1442999.
 37. Kudo Y, Haymaker C, Zhang J, Reuben A, Duose DY, Fujimoto J, Roy-Chowdhuri S, Solis Soto LM, Dejima H, Parra ER, et al. Suppressed immune microenvironment and repertoire in brain metastases from patients with resected non-small-cell lung cancer. *Ann Oncol.* 2019;30(9):1521–1530. doi:10.1093/annonc/mdz207.

38. Mansfield AS, Ren H, Sutor S, Sarangi V, Nair A, Davila J, Elsbernd LR, Udell JB, Dronca RS, Park S, et al. Contraction of T cell richness in lung cancer brain metastases. *Sci Rep.* 2018;8(1):2171. doi:10.1038/s41598-018-20622-8.
39. Coffelt SB, Wellenstein MD, de Visser KE. Neutrophils in cancer: neutral no more. *Nat Rev Cancer.* 2016;16(7):431–446. doi:10.1038/nrc.2016.52.
40. Venet F, Monneret G. Advances in the understanding and treatment of sepsis-induced immunosuppression. *Nat Rev Nephrol.* 2018;14(2):121–137. doi:10.1038/nrneph.2017.165.
41. Christoffersson G, Vågesjö E, Vandooren J, Lidén M, Massena S, Reinert RB, Brissova M, Powers AC, Opendakker G, Phillipson M, et al. VEGF-A recruits a proangiogenic MMP-9-delivering neutrophil subset that induces angiogenesis in transplanted hypoxic tissue. *Blood.* 2012;120(23):4653–4662. doi:10.1182/blood-2012-04-421040.
42. Zhou SL, Zhou Z-J, Hu Z-Q, Huang X-W, Wang Z, Chen E-B, Fan J, Cao Y, Dai Z, Zhou J, et al. Tumor-Associated Neutrophils Recruit Macrophages and T-Regulatory Cells to Promote Progression of Hepatocellular Carcinoma and Resistance to Sorafenib. *Gastroenterology.* 2016;150(7):1646–1658.e17. doi:10.1053/j.gastro.2016.02.040.
43. Tecchio C, Cassatella MA. Neutrophil-derived chemokines on the road to immunity. *Semin Immunol.* 2016;28(2):119–128. doi:10.1016/j.smim.2016.04.003.
44. Mitsuya K, Nakasu Y, Kurakane T, Hayashi N, Harada H, Nozaki K. Elevated preoperative neutrophil-to-lymphocyte ratio as a predictor of worse survival after resection in patients with brain metastasis. *J Neurosurg.* 2017;127(2):433–437. doi:10.3171/2016.8.JNS16899.
45. Zhang L, Hu Y, Chen W, Tian Y, Xie Y, Chen J. Pre-stereotactic radiosurgery neutrophil-to-lymphocyte ratio is a predictor of the prognosis for brain metastases. *J Neurooncol.* 2020;147(3):691–700. doi:10.1007/s11060-020-03477-w.
46. Lin YJ, et al. Roles of Neutrophils in Glioma and Brain Metastases. *Front Immunol.* 2021;12:701383. doi:10.3389/fimmu.2021.701383.
47. Goldberg SB, Schalper KA, Gettinger SN, Mahajan A, Herbst RS, Chiang AC, Lilenbaum R, Wilson FH, Omay SB, Yu JB, et al. Pembrolizumab for management of patients with NSCLC and brain metastases: long-term results and biomarker analysis from a non-randomised, open-label, phase 2 trial. *Lancet Oncol.* 2020;21(5):655–663. doi:10.1016/S1470-2045(20)30111-X.
48. Schmid TE, Multhoff G. Radiation-induced stress proteins - the role of heat shock proteins (HSP) in anti- tumor responses. *Curr Med Chem.* 2012;19(12):1765–1770. doi:10.2174/092986712800099767.
49. Berghoff AS, Lassmann H, Preusser M, Höftberger R. Characterization of the inflammatory response to solid cancer metastases in the human brain. *Clin Exp Metastasis.* 2013;30(1):69–81. doi:10.1007/s10585-012-9510-4.
50. Deng L, Liang H, Burnette B, Beckett M, Darga T, Weichselbaum RR, Fu Y-X. Irradiation and anti-PD-L1 treatment synergistically promote antitumor immunity in mice. *J Clin Invest.* 2014;124(2):687–695. doi:10.1172/JCI67313.
51. Dovedi SJ, et al. Acquired resistance to fractionated radiotherapy can be overcome by concurrent PD-L1 blockade. *Cancer Res.* 2014;74(19):5458–5468. doi:10.1158/0008-5472.CAN-14-1258.
52. Rudqvist NP, Pilonis KA, Lhuillier C, Wennerberg E, Sidhom J-W, Emerson RO, Robins HS, Schneck J, Formenti SC, Demaria S, et al. Radiotherapy and CTLA-4 Blockade Shape the TCR Repertoire of Tumor-Infiltrating T Cells. *Cancer Immunol Res.* 2018;6(2):139–150. doi:10.1158/2326-6066.CIR-17-0134.
53. Emens LA, Middleton G. The interplay of immunotherapy and chemotherapy: harnessing potential synergies. *Cancer Immunol Res.* 2015;3(5):436–443. doi:10.1158/2326-6066.CIR-15-0064.
54. Fares J, et al. Emerging principles of brain immunology and immune checkpoint blockade in brain metastases. *Brain.* 2021. doi:10.1093/brain/awab012.
55. Jiang T, Cheng R, Pan Y, Zhang H, He Y, Su C, Ren S, Zhou C. Heterogeneity of neoantigen landscape between primary lesions and their matched metastases in lung cancer. *Transl Lung Cancer Res.* 2020;9(2):246–256. doi:10.21037/tlcr.2020.03.03.
56. Shibutani M, Maeda K, Nagahara H, Fukuoka T, Matsutani S, Kashiwagi S, Tanaka H, Hirakawa K, Ohira M. A comparison of the local immune status between the primary and metastatic tumor in colorectal cancer: a retrospective study. *BMC Cancer.* 2018;18(1):371. doi:10.1186/s12885-018-4276-y.
57. Goto R, Hirota Y, Aruga T, Horiguchi S, Miura S, Nakamura S, Takimoto M. The number of FoxP3-positive tumor-infiltrating lymphocytes in patients with synchronous bilateral breast cancer. *Breast Cancer.* 2020;27(4):586–593. doi:10.1007/s12282-020-01049-4.
58. Chen TC, et al. The differences of immunologic and TP53 mutant phenotypes between synchronous and metachronous head and neck cancer and esophageal cancer. *Oral Oncol.* 2020;111:104945. doi:10.1016/j.oraloncology.2020.104945.
59. van den Ende T, et al. Priming the tumor immune microenvironment with chemo(radio)therapy: a systematic review across tumor types. *Biochim Biophys Acta Rev Cancer.* 2020;1874(1):188386. doi:10.1016/j.bbcan.2020.188386.
60. Dominguez C, Tsang KY, Palena C. Short-term EGFR blockade enhances immune-mediated cytotoxicity of EGFR mutant lung cancer cells: rationale for combination therapies. *Cell Death Dis.* 2016;7(9):e2380. doi:10.1038/cddis.2016.297.
61. Kelly RJ, Zaidi AH, Smith MA, Omstead AN, Kosovec JE, Matsui D, Martin SA, DiCarlo C, Werts ED, Silverman JF, et al. The Dynamic and Transient Immune Microenvironment in Locally Advanced Esophageal Adenocarcinoma Post Chemoradiation. *Ann Surg.* 2018;268(6):992–999. doi:10.1097/SLA.0000000000002410.
62. Jia Y, Li X, Jiang T, Zhao S, Zhang L, Liu X, Shi J, Qiao M, Luo J, et al. EGFR-targeted therapy alters the tumor microenvironment in EGFR-driven lung tumors: implications for combination therapies. *Int J Cancer.* 2019;145(5):1432–1444. doi:10.1002/ijc.32191.
63. Isomoto K, Haratani K, Hayashi H, Shimizu S, Tomida S, Niwa T, Yokoyama T, Fukuda Y, Chiba Y, Kato R, et al. Impact of EGFR-TKI Treatment on the Tumor Immune Microenvironment in EGFR Mutation-Positive Non-Small Cell Lung Cancer. *Clin Cancer Res.* 2020;26(8):2037–2046. doi:10.1158/1078-0432.CCR-19-2027.
64. Park YH, Lal S, Lee JE, Choi Y-L, Wen J, Ram S, Ding Y, Lee S-H, Powell E, Lee SK, et al. Chemotherapy induces dynamic immune responses in breast cancers that impact treatment outcome. *Nat Commun.* 2020;11(1):6175. doi:10.1038/s41467-020-19933-0.